Proc. Natl. Acad. Sci. USA
Vol. 79, pp. 5001–5005, August 1982
Ecology

Microscale nutrient patches produced by zooplankton

(autoradiography/phosphate uptake/phytoplankton)

JOHN T. LEHMAN*† AND DONALD SCAVIA*‡

*Division of Biological Sciences and †Great Lakes Research Division, Natural Science Building, The University of Michigan, Ann Arbor, Michigan 48109; and ‡National Oceanic and Atmospheric Administration, Great Lakes Environmental Research Laboratory, 2300 Washtenaw Avenue, Ann Arbor, Michigan 48104

Communicated by W. T. Edmondson, May 10, 1982

ABSTRACT **Both track autoradiography and grain-density autoradiography show that individual zooplankton create miniature patches of dissolved nutrients and that algae exploit those regions to absorb phosphate. The patches are short lived and can be dispersed artificially by small-scale turbulence. Our data support a simple model of encounters between algae and nutrient plumes produced by swimming zooplankton.**

Ambient concentrations of P_i can defy limits of detection in productive surface waters of lakes and oceans. Even the traces measured chemically often overestimate by an order of magnitude or more the pool of P_i that is most readily used by the algae (1–3). We find an incongruence between these field observations and kinetic data on P_i use by algae. The P_i concentrations reported from nature often seem insufficient to support measured rates of primary production and cell division, particularly during summer. Half-saturation constants reported for steady-state growth of lake phytoplankton range from 6 nM to about 300 nM (4, 5). Radiochemical assays, on the other hand, show that maximal P_i concentrations in some lakes rarely exceed 3 nM during summer (6). Only minute fractions of maximal growth rates could be supported by such low concentrations.

Rapid growth at those low concentrations is even less likely, judging from theoretical and experimental demonstrations of threshold concentrations for P_i in the nanomolar range, below which net uptake is zero (7, 8). In fact, the radiochemical assay used to determine P_i concentration shows that efflux of P_i from cells virtually equals influx at ambient concentrations (see, e.g., ref. 2). Moreover, there are physical limits to uptake rates that are dictated by nutrient diffusion (9, 10). At bulk concentrations close to zero, it is difficult to establish the concentration gradients needed to support high fluxes to the cells. Because biotic uptake of P_i is an enzyme-mediated process, concentrations at the cell boundary must be nonzero but lower than bulk concentrations (11, 12).

Despite these obstacles, lake phytoplankton survive and grow all through the summer. We think the apparent inconsistency stems from traditional notions about homogeneity in aquatic environments. Perhaps algae do not compete in nature for constant low concentrations of nutrients.

Nutrients released from crustacean zooplankton are the major source to phytoplankton in some lakes during summer (13). It has been hypothesized that zooplankton create nutrient patches that are exploited by algae (14), but that claim has been attacked with mathematical models (15, 16). We recently demonstrated that nutrient patches do exist. In the presence of zooplankton labeled with ^{33}P, algae become labeled differentially unless the solution is stirred rapidly (17). We used track autoradiography to quantify the distribution of radiotracer among algal cells. Another technique, grain-density autoradiography, can be used for equally critical quantitative analyses. Here we describe that alternative approach, and we derive a patch–encounter model that is consistent with all of our data.

The publication costs of this article were defrayed in part by page charge payment. This article must therefore be hereby marked "*advertisement*" in accordance with 18 U. S. C. §1734 solely to indicate this fact.

METHODS

All cultures were grown and experiments were conducted at 20°C. *Ankistrodesmus falcatus* and *Chlamydomonas reinhardti* were grown axenically in MWC culture medium (18). *Daphnia pulex* were raised in filtered aged Ann Arbor tap water and were fed *Ankistrodesmus*. Two days before an experiment, an aliquot of an *Ankistrodesmus* culture was concentrated by centrifugation and ca. 2 mCi of $^{33}P_i$ (1 Ci = 3.7×10^{10} becquerels) was added. After 10 min, the radioactive mixture was added to 2 liters of freshly filtered epilimnetic water from Third Sister Lake, Michigan. Approximately 30 adult female *Daphnia* (2 mm long) were added and they fed for 2 days, achieving body burdens in excess of 5 μCi.

Also 2 days before an experiment, 250 ml of a *Chlamydomonas* culture was centrifuged aseptically and the cells were suspended in 1.5 liters of MWC medium without P_i. After 2 days, the cell suspension was diluted to ca. 10^5 cells/ml with a sterile mineral medium containing $CaCl_2 \cdot 2H_2O$, $MgSO_4$, and $NaHCO_3$, each at 40 mg/liter. Samples were taken after dilution for cell counts and for determinations of chlorophyll *a* and phosphorus (19, 20).

Kinetics of P_i Uptake. Aliquots of 100 ml were dispensed from the experimental cultures of *Chlamydomonas* to 250-ml Erlenmeyer flasks, magnetic stirring bars were added, and each flask was placed on a mixing device at 45.5 (microeinsteins/m^2)/sec (400–700 nm) illumination from 40 W cool white fluorescent bulbs. Aliquots of a sterile solution containing 0.1 μmol of P_i and $^{33}P_i$ at ca. 20 μCi/ml were added to the flasks to produce a range of P_i additions from 10 nM to 1 μM. One flask received carrier-free $^{33}P_i$ only. At 2-min intervals, a 5-ml aliquot was withdrawn from each flask and the cells were collected on 0.45-μm Millipore filters previously soaked in 1 mM KH_2PO_4. Filters were rinsed with 2 to 3 ml of cell-free nonradioactive culture medium and were transferred to scintillation vials with 10 ml of ACS (Amersham); radioactivity was assayed on a Beckman LS-230 optimized for ^{33}P. Adsorption of $^{33}P_i$ to the filters was minimal but was assessed by using "blank" filters placed under the filters used to collect cells.

Each uptake treatment mixture was sampled for 12–15 min and then 1 ml of the suspension was placed in a scintillation vial to verify the precise quantity of radiotracer (and thus P_i concentration) used. Time courses were plotted and, if necessary, only the initial linear portion of the plot was used to calculate uptake rate.

Nutrient Patch Experiments. Aliquots of 300 ml from the experimental *Chlamydomonas* culture were dispensed into 400-ml beakers. $^{33}P_i$-labeled *Daphnia* were used as nutrient sources

to these algae in stirred and unstirred mixtures as described (17). After 30 min, the contents of each experimental beaker was poured through a sieve, which retained the *Daphnia*, into beakers containing 1 ml of acid/Lugol's preservative (21). One-milliliter aliquots were withdrawn immediately from the preserved samples and filtered through 24-mm-diameter 0.22-μm Millipore filters. Filters were rinsed as in the uptake experiments and placed while damp on glass slides previously cleaned in dichromic acid, washed vigorously, and then dipped in a gelatin/chrome alum subbing solution (22).

Autoradiography. Slides with attached filters were dried overnight at room temperature and then cleared over boiling acetone. For grain-density autoradiography, the slides were used directly but, for track autoradiography, the slides were dipped once more in subbing solution and then dried.

For grain-density autoradiography, we dipped the slides in Kodak NTB3 emulsion at 43°C; for track autoradiography, we worked at 28°C. We used established procedures with D-19 as the developer (22, 23) and all solutions were held at 18°C. Coverslips were mounted with glycerine and counts were made at ×720 or ×1,080 on an Olympus BH microscope using interference contrast optics. For grain counts, all silver grains within one cell diameter of individual cells were recorded. Control slides prepared with nonradioactive *Chlamydomonas* were used to assess background counts. Background track counts were virtually zero.

RESULTS AND DISCUSSION

The distribution of background grains per cell is adequately described by a Poisson model ($P = 0.35$), but the distributions of grains per cell for experimental treatments definitely are not ($P < 10^{-10}$), based on χ^2 goodness-of-fit tests. Although the number of radioactive disintegrations per cell must follow a Poisson distribution when the cells contain identical quantities of radioisotope, the individual β-particle tracks arising from the disintegrations expose various numbers of grains in the thin layer of emulsion. The number depends on the initial energy of each β-particle, the initial orientation of the track, and the thickness of the emulsion.

We presume that the distribution of grains per track conforms to a Poisson model, which means that the observed grains per cell represents a composite of two Poisson processes. The composite distribution is called Neyman's type A (24) and it is characterized by two parameters, the mean and the ratio of the variance to the mean. This distribution does in fact fit the stirred mixture but not the unstirred mixture (Fig. 1). Adherence to the model implies that all of the cells contain identical quantities of radioisotope. With stirring, ^{33}P released from the animals is equally exploited by the algal cells. Failure of the unstirred mixture to conform to the model guarantees that the algae are labeled differentially. The differential labeling is reflected in the greater skewness of the frequency distribution of the unstirred mixture (1.318) compared with the stirred mixture (0.619). The finding confirms our report based on frequency distributions of β-particle tracks in independent experiments (17).

Because P_i released from swimming *Daphnia* is not equally accessible to all algae unless the solution is stirred, the true distribution of ^{33}P per cell in the unstirred mixtures is important. We have taken two approaches to determine that distribution, both of which conform with our data but differ substantially in conceptual and mathematical complexity.

Nutrient Plume Model. Following previous workers (15, 16), we assembled a model for nutrients released by animals and then coupled it to the uptake physiology of the algae. We consider a nutrient source (the animal) at the origin moving at velocity u in the $-x$ direction. The nutrient plume behind the animal is given in cylindrical coordinates by the solution to

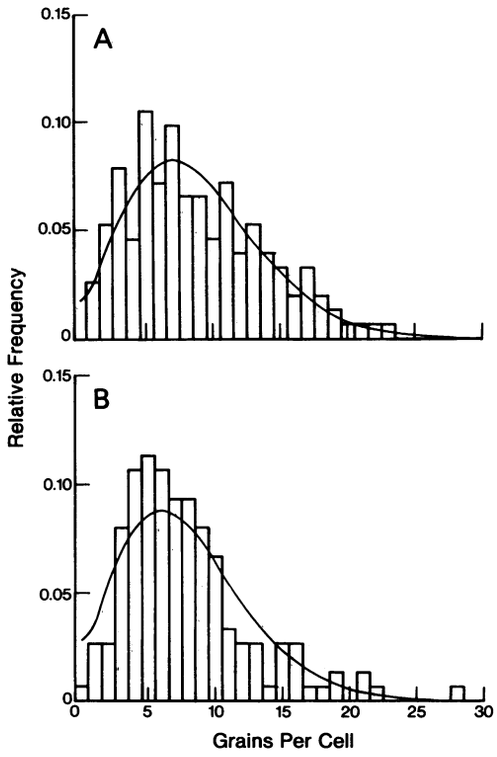

FIG. 1. Frequency distributions of grains per cell for the stirred mixture (A; $n = 152$) and the unstirred mixture (B; $n = 150$). Data are presented as histograms; the smooth curves represent Neyman's type A distributions with mean and variance equal to sample distributions. The model distribution fits the stirred mixture ($P = 0.865$, $\chi^2 = 14.9$, df = 22) but not the unstirred mixture ($P = 0.0115$, $\chi^2 = 46.4$, df = 27). Goodness of fit was based on a χ^2 test with $N - 2$ degrees of freedom (df) where N is the number of histogram cells. Statistics are based on absolute frequencies.

$$\frac{\partial c}{\partial t} = -u\frac{\partial c}{\partial x} + D\left[\frac{1}{r}\frac{\partial}{\partial r}\left(r\frac{\partial c}{\partial r}\right) + \frac{\partial^2 c}{\partial x^2}\right], \quad [1]$$

with r measured radially from the path of the swimming animal. D is the diffusion coefficient, t is time, and c is concentration. With appropriate boundary constraints, the solution at steady state (25) is

$$c = (Q/4\pi Ds)e^{-u(s-x)/2D}, \quad [2]$$

where $s^2 = x^2 + r^2$. Q is the rate of nutrient release per animal. Numerical values were chosen to correspond to 2-mm adult female *Daphnia pulex*: $Q = 0.0618$ pmol of P per animal per sec (26); $u = 0.15$ cm/sec (27); $D = 10^{-5}$ cm^2/sec (molecular diffusion). The assumption of molecular diffusion is appropriate for the Reynold's numbers and drag regimes experienced by *Daphnia* (17). Contours of resulting P_i concentrations are plotted in Fig. 2*A*.

Fig. 2*A* applies to an animal in water without algae; algal cells alter the nutrient regime by absorbing P_i. The uptake physiology of *Chlamydomonas* for P_i was measured in conjunction with each experiment; measured parameters are listed in Table 1. Our preliminary calculations showed that the algae in our experiments could absorb a sizable fraction, if not all, of the P_i released by the animals. Biological uptake by algae, as well as physical dispersion, controls the actual distribution and abundance of P_i behind an animal. By incorporating the uptake phys-

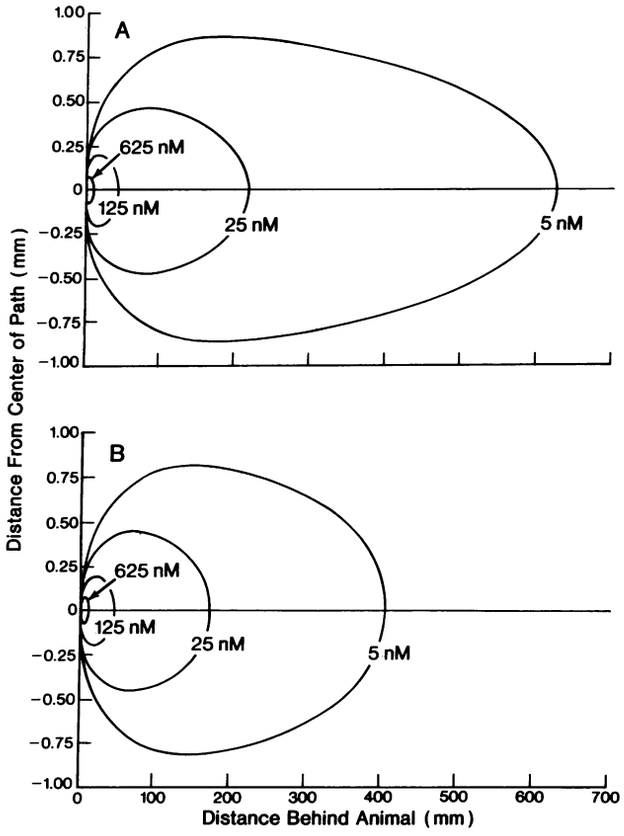

FIG. 2. (*A*) Contour diagram for the steady-state plume of P_i behind a swimming *Daphnia pulex* calculated from Eq. 2. (*B*) Contour diagram with algal uptake of P_i included from Eq. 3.

iology of the algae, changes in nutrient concentration are more properly described by

$$\frac{\partial c}{\partial t} = -u\frac{\partial c}{\partial x} + D\left[\frac{1}{r}\frac{\partial}{\partial r}\left(r\frac{\partial c}{\partial r}\right) + \frac{\partial^2 c}{\partial x^2}\right] - \left[\frac{V_{max}\cdot c}{K_m + c}\right]N, \quad [3]$$

where V_{max} is the maximum uptake rate, K_m is the half-saturation constant for uptake (Table 1), and N is the concentration of algal cells (ca. 10^5/ml in our experiments).

The domain of integration for net uptake (the last term in Eq. 3) was confined to P_i concentrations greater than or equal to a finite threshold. Using radiobioassay techniques (2), we determined that the threshold concentration for positive net uptake of P_i was 5 nM in our experiments. We could not obtain an analytical solution for Eq. 3 so we prepared a numerical simulation in cylindrical coordinates. Finite differences were taken as forward in time (Δt = 0.1 sec) and backward in space (Δx = 0.15 cm, Δr = 0.002 cm). The steady state solution achieved after 700 simulated sec (Fig. 2*B*) shows that the contours of P_i concentration inside the plume envelop a much smaller volume than they would if the algae were not present (i.e., Fig. 2*A*).

Table 1. Physiological parameters for P_i uptake by *Chlamydomonas* measured in the grain-density autoradiography experiment (Grain) and in a track autoradiography experiment (Track)

	V_{max}, 0.01 fmol of P per cell per min	K_m, nM P	Cell quota, fmol of P per cell
Grain	14.6 (12.5–16.8)	80.1 (45.8–114.5)	2.32
Track	8.5 (7.5– 9.6)	27.3 (8.6– 45.9)	2.42

V_{max}, maximum uptake rate. Values in parentheses are 95% confidence limits.

Algal cells different radial distances from an animal experience different nutrient regimes through time and they obtain different quantities of P_i. We calculated integrated net uptake of P at each radius r_i from the animal's path from concentrations within the volume elements used to obtain the numerical solution shown in Fig. 2*B*. From these values, we constructed the predicted frequency distribution for the total mass of P absorbed by algae during one encounter (Fig. 3). We used a cubic spline function to express r in terms of simulated net uptake (U). Perpendicular to the center line of the nutrient plume, we presume that algal cells are distributed in space proportional to $2\pi r$ (i.e., the suspension is homogeneous). We thus calculated the frequency distribution of U as proportional to $2\pi r\partial r/\partial U$.

The frequency distribution in Fig. 3 pertains only to cells that have encountered a nutrient plume. Some algae were never close enough to a passing animal to experience concentrations above the threshold for net uptake. In fact, we intentionally kept the experiments short to guarantee that many algae would fit that category. We consequently assume that the empirical mean radioactivity per cell quantified in our experiments is a result of some fraction (f) of the population having obtained ^{33}P as in Fig. 3 and the remaining fraction ($1 - f$) having remained unlabeled. The average amount of ^{33}P in the labeled cells would be $\bar{X}/f$ where $\bar{X}$ is the average number of disintegrations per cell measured for the whole population from autoradiographs.

Comparison between model prediction and empirical data is most direct using our results from track autoradiography (17), because β-particle tracks represent individual nuclear disintegrations. If all cells contain equal amounts of $^{33}P_i$, the frequency distribution of tracks per cell will follow the Poisson distribution:

$$P_j = \frac{\lambda^j}{j!}e^{-\lambda}, \quad [4]$$

where λ is mean tracks per cell generated by that constant amount of isotope. If cells do not contain equal amounts of isotope, the basic distribution still follows the Poisson model (Eq. 4), but the parameter λ becomes a variable representing the mean number of tracks expected for each different amount of ^{33}P per cell. The model then becomes a summation of many weighted Poisson distributions, each having a mean value and weight drawn from the distribution of ^{33}P per cell. In the special case in which λ is also distributed as a Poisson variable, the re-

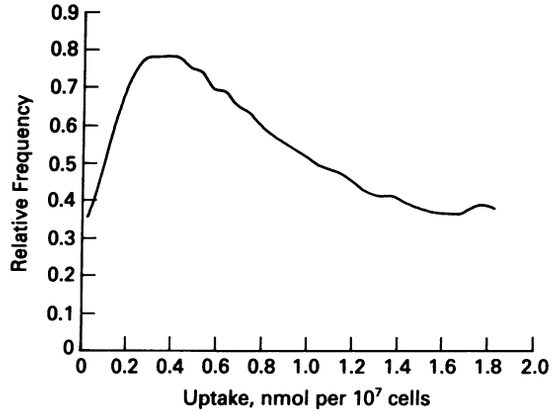

FIG. 3. Frequency distribution of net uptake of P for algal cells that encounter a nutrient plume. The distribution was constructed by numerical methods using the nutrient plume model.

sulting distribution is Neyman's type A as discussed above for grains per cell.

We first transformed the domain of the calculated frequency distribution for uptake by cells that encountered a plume (Fig. 3) from nanomoles (U) to disintegrations (X) by multiplying by $(\overline{X}/f)/\overline{U}$ where $\overline{U}$ is the calculated mean mass uptake. Then the frequencies (F_i) were multiplied by a fraction (f) to account for cells that encountered the plume; the remaining ($1 - f$) frequency was assigned to $X = 0$ ($F_0 = 1 - f$). The predicted distribution of β-particle tracks (T_j) was derived numerically as a weighted cumulative Poisson distribution:

$$T_j = \sum_i \frac{F_i(X_i)^j}{j!} e^{-X_i}. \quad [5]$$

The predicted distribution is given in Table 2. It is compared with the distribution of β-particle tracks per cell that we observed in an unstirred mixture with zooplankton present (17). We reported in that study that observed distributions for stirred mixtures conform to Poisson models but, as we show in Table 2, the unstirred mixture does not ($P < 10^{-7}$). The data are not inconsistent with Poisson processes, however, because by applying our plume model with $f = 0.38$ (the best fit), our predictions are statistically indistinguishable from the observed distribution ($P = 0.38$). According to this nutrient plume model, cells do not contain identical amounts of radiophosphorus; rather, the quantity of ^{33}P per cell varies in proportion to the frequency distribution shown in Fig. 3.

Simple Encounter Model. Although the model developed above is appealing because of its mechanistic details, it ignores important features of zooplankton behavior. The animals move discontinuously, and their feeding currents allow them to contact considerable volumes of water even when they are stationary. Some cells are ingested and do not subsequently contribute to the observed frequency distributions. Rather than elaborate the model with these processes, an alternative and simpler view can be tested. We hypothesize that what is most important is whether or not a cell encounters a nutrient patch and survives. Differences among cells that do encounter a patch may be insignificant compared with the difference it makes to have experienced the elevated nutrient regime at all. Our alternative model presumes that the population of algae in our experiments consists of two groups: one group that has never encountered a patch and has no detectable ^{33}P and one group that has had an encounter and all contain a fixed mass of ^{33}P ($\overline{X}/f$). The predicted frequency distribution for this model was calculated by using Eq. 5 with $F_0 = 1 - f$ and $F_X = f$; predictions are given in Table 2. For $f = 0.31$ (the best fit), this simple encounter model is statistically indistinguishable from the data ($P = 0.40$) and from the more complex nutrient plume model ($P = 0.92$).

Identical conclusions can be reached by using grain distributions. If we assume that grains per track follows a Poisson process, a second summation of Poisson models with parameter (γj) representing mean grains per track (γ) times j tracks per cell (distributed as T_j; Eq. 5) results in the expected distribution of grains per cell that arise from the tracks of β-particles (β_i):

$$\beta_i = \sum_j \frac{T_j(\gamma j)^i}{i!} e^{-\gamma j}. \quad [6]$$

This distribution must further be modified to incorporate the frequencies of background grains that conform to a Poisson model. The predicted distribution of grains per cell (G_i) is thus a convolution of the background distribution and the distribution of grains arising from real tracks:

$$G_i = \sum_{j=0}^{i} \beta_{i-j} \cdot \frac{B^j}{j!} e^{-B}, \quad [7]$$

where B is the mean number of background grains per cell. We made no effort to find a "best fit" to the unstirred grain distribution (Fig. 1). For $\overline{X} = 1.5$ disintegrations per cell, $\gamma = 2$ grains per track, $B = 5$ grains per cell, and $f = 0.4$ of the population encountering a nutrient patch, both the nutrient plume model and the simple encounter model produce predictions that are statistically indistinguishable from the observed distribution ($P = 0.69$ and 0.62, respectively). This again demonstrates the heterogeneity of nutrient supply and reinforces our claim that frequencies of encounter influence the results more than do the relative amounts of nutrient that cells obtain during an encounter.

Following the logic of Eqs. 5–7, a correction for background grains should be applied even to stirred mixtures. The adequate fit we obtained to Neyman's type A distribution for the unstirred mixture (Fig. 1) shows that the correction is not essential at levels we can resolve. Incorporating a background distribution numerically, as in Eq. 7 where β_i is a Neyman's type A distribution, did not change the shape of the predicted grain distribution noticeably.

Our results and conclusions apply to conditions in which molecular diffusion dominated and only one species of alga was present. In nature, the shapes of nutrient patches depend on the magnitude of physical dispersion and on the abundances and kinetic properties of the various species present. Turbulence generated at large space scales in lakes and oceans effectively dissipates without changing the distribution of materials at millimeter scales (17). Therefore, if turbulence were present in nature on the scales considered here, it would have to be generated by zooplankton. Much evidence, primarily from microcinematography (28–31), demonstrates that fluid flow associated with feeding and swimming motions of marine and freshwater zooplankton is laminar. In that viscous environment, it would be impossible to generate turbulence. Thus, extrapolating our results to nature is certainly not unwarranted on that account.

The presence of nutrient-enriched microenvironments in nature can alter the mechanisms controlling competition for nutrient resources. The patches may be particularly important after the vernal bloom period when bulk concentrations of nutrients are low and recycled nutrients are important. In our experiments, almost all ^{33}P released by animals was absorbed by algae whether the vessel was stirred or not. We therefore do not presume that patchy nutrient environments are necessarily any more beneficial to algae than are uniform ones. But the fact of nutrient patchiness may create different selective pressures than would homogeneous environments. To evaluate the outcome of interspecific competition when limiting nutrients are present only in temporary patches, the relative abil-

Table 2. Frequency distribution of β-particle tracks per cell for the unstirred mixture in a track autoradiography experiment

Tracks per cell	Observed	Predicted		
		Poisson	Plume*	Encounter†
0	248	233.6	249.8	248.5
1	32	58.4	32.4	33.5
2	17	7.3	12.4	13.5
3	3	0.6	3.9	3.6
4	0	0.04	1.1	0.7
χ^2		35.10	1.91	1.81
P (df = 2)		2.4×10^{-8}	0.38	0.40

*$f = 0.38$.
†$f = 0.31$.

ities of different species to absorb quickly and store the nutrients are most important. The patchiness we describe here would favor species that increase their cell nutrient quotas most during an encounter. This puts a premium on maximal rates of nutrient uptake rather than strictly on abilities to acquire nutrients at low concentrations outside the patches where, in fact, concentrations may be virtually zero.

We thank W. S. Gardner, L. R. Herche, J. A. Robbins, S. J. Tarapchak, and H. A. Vanderploeg for helpful discussions and for comments on the manuscript. D. A. Lehman provided technical assistance. This study was supported in part by National Science Foundation Grant DEB79-22143. This is contribution no. 290 from the Great Lakes Environmental Research Laboratory and contribution no. 335 from the Great Lakes Research Division.

1. Kuenzler, E. J. & Ketchum, B. H. (1962) *Biol. Bull. (Woods Hole, MA)* **123,** 134–145.
2. Rigler, F. H. (1966) *Verh.-Int. Ver. Theor. Angew. Limnol.* **16,** 465–470.
3. Brown, E. J., Harris, R. F. & Koonce, J. F. (1978) *Limnol. Oceanogr.* **23,** 26–34.
4. Ahlgren, G. (1978) *Mitt. Int. Ver. Theor. Angew. Limnol.* **21,** 88–102.
5. Kilham, S. S. (1978) *Mitt. Int. Ver. Limnol.* **21,** 147–157.
6. Levine, S. N. & Schindler, D. W. (1980) *Can. J. Fish. Aquat. Sci.* **37,** 479–487.
7. Button, D. K. (1978) *Deep-Sea Res. Oceanogr. Abstr.* **25,** 1163–1177.
8. Brown, E. J. & Button, D. K. (1979) *J. Phycol.* **15,** 305–311.
9. Harvey, H. W. (1937) *J. Mar. Biol. Assoc. U. K.* **22,** 205–219.
10. Munk, W. H. & Riley, G. A. (1952) *J. Mar. Res.* **11,** 215–240.
11. Pasciak, W. & Gavis, J. (1974) *Limnol. Oceanogr.* **19,** 881–888.
12. Gavis, J. (1976) *J. Mar. Res.* **34,** 161–179.
13. Lehman, J. T. (1980) in *Evolution and Ecology of Zooplankton Communities,* ed. Kerfoot, W. C. (Univ. Press of New England, Hanover, NH), Am. Soc. Limnol. Oceanogr. Spec. Symp. 3, pp. 251–263.
14. Goldman, J. C., McCarthy, J. J. & Peavey, D. G. (1979) *Nature (London)* **279,** 210–215.
15. Jackson, G. A. (1980) *Nature (London)* **284,** 439–441.
16. Williams, P. J. L. & Muir, L. R. (1981) in *Ecohydrodynamics,* ed. Nihoul, J. C. J. (Elsevier/North–Holland, New York) Elsevier Oceanography Series, 32, pp. 209–218.
17. Lehman, J. T. & Scavia, D. (1982) *Science* **216,** 729–730.
18. Lehman, J. T. (1976) *J. Phycol.* **12,** 190–193.
19. Strickland, J. D. H. & Parsons, T. R. (1972) *A Practical Handbook of Seawater Analysis* (Bull. Fish. Res. Bd., Canada), 2nd Ed., p. 185.
20. Menzel, D. & Corwin, N. (1965) *Limnol. Oceanogr.* **10,** 280–282.
21. Lind, O. T. (1979) *Handbook of Common Methods in Limnology* (Mosby, St. Louis, MI), 2nd Ed., p. 109.
22. Rogers, A. W. (1979) *Techniques of Autoradiography* (Elsevier/North–Holland, New York), 2nd Ed.
23. Knoechel, R. & Kalff, J. (1976) *Limnol. Oceanogr.* **21,** 590–595.
24. Johnson, N. L. & Kotz, S. (1969) *Discrete Distributions* (Houghton Mifflin, Boston), p. 216.
25. Bird, R. B., Stewart, W. E. & Lightfoot, E. N. (1960) *Transport Phenomena* (Wiley, New York), p. 552.
26. Lehman, J. T. (1980) *Limnol. Oceanogr.* **25,** 620–632.
27. Gerritsen, J. (1980) in *Evolution and Ecology of Zooplankton Communities,* ed. Kerfoot, W. C. (Univ. Press of New England, Hanover, NH), Am. Soc. Limnol. Oceanogr. Spec. Symp. 3, pp. 52–62.
28. Kerfoot, W. C., Kellog, D. C. & Strickler, J. R. (1980) in *Evolution and Ecology of Zooplankton Communities,* ed. Kerfoot, W. C. (Univ. Press of New England, Hanover, NH), Am. Soc. Limnol. Oceanogr. Spec. Symp. 3, pp. 10–27.
29. Alcaraz, M., Paffenhofer, G. A. & Strickler, J. R. (1980) in *Evolution and Ecology of Zooplankton Communities,* ed. Kerfoot, W. C. (Univ. Press of New England, Hanover, NH), Am. Soc. Limnol. Oceanogr. Spec. Symp. 3, pp. 241–248.
30. Lehman, J. T. (1977) *Limnol. Oceanogr.* **22,** 170–172.
31. Koehl, M. A. R. & Strickler, J. R. (1981) *Limnol. Oceanogr.* **26,** 1062–1073.